Nonlinearity and trapping in excitation transfer: Dimers and trimers

Ivan Barvík*
Institute of Physics, Charles University, Ke Karlovu 5, 121 16 Prague, Czech Republic

Bernd Esser and Holger Schanz†
Institute of Physics, Humboldt University, Invalidenstrasse 110, 10 099 Berlin, Germany
(Received 19 September 1994; revised manuscript received 17 April 1995)

We study the interplay between nonlinearity in exciton transport and trapping due to a sink site for the dimer and a chain trimer by a numerical integration of the discrete nonlinear Schrödinger equation. Our results for the dimer show, that the formation of a self-trapped state due to the nonlinear coupling increases the lifetime of the exciton substantially. Self-trapping can be enhanced by the sink for short times, but for long times it disappears due to the presence of the sink. In the trimer consisting of a subdimer extended by a sink site there exists a transition between states localized on the two sites of the subdimer before for larger nonlinear coupling self-trapping on one site of the subdimer is observed. Very large trapping rates lead to an increasing lifetime of the excitation on both the dimer and the trimer. The sink site is then effectively decoupled. We explain this effect using an asymptotic theory for strong trapping and demonstrate it by numerical computation.

I. INTRODUCTION

The purpose of this paper is to study the interplay between a coherent transfer regime of an exciton and the two processes leading to the loss of the linear character of the exciton transfer, namely trapping of the particle and transport nonlinearity. The system under study is a moving quasiparticle interacting strongly with polarization vibrations. At one of the sites of the configuration trapping with a prescribed rate γ can occur. Although the influences of nonlinearity and trapping on transport properties have been investigated separately in detail, the combination of both, which can be important in the application of transfer theory, has not yet been quantitatively evaluated.

Trapping of quasiparticles constitutes an important phenomenon in many areas of physics. In photosynthesis, for instance, an exciton in a harvesting antenna transfers its energy to a reaction center, where it can be trapped. Electron transfer processes then follow. Having in mind systems of this kind, the initial conditions are chosen throughout this paper such that the excitation is initially located outside the sink site.

Much work has been done on the exciton transfer theories in the last decades. Beginning with the microscopic treatment by Haken and Reineker[1] and Grover and Silbey[2] a number of theories such as the general master equation (GME),[3] the stochastic Liouville equation (SLE),[4] the Pauli master equation,[5] and the continuous time random walk[6] (CTRW) were developed and mainly directed to obtaining equations which describe the coupled coherent and incoherent motion of the excitation. Only recently[7–12] the problem of a rigorous description, leading to positive occupation probabilities of the trap (modeled as a sink) in the coherent and near coherent regimes of the excitation transfer has been solved using the GME, SLE, and CTRW methods.

Using the SLE,[9,10] it was shown for more extended systems that an excitation generated outside the sink site behaves as though it would like to avoid this site. This effect has been observed also in the case of a semi-infinite linear chain[11] and results in an effective decoupling of the sink site from the rest of the configuration. In this case the decay of the whole occupation probability $P(t)$ with time is slower for larger γ. In particular, in a linear trimer with a sink introduced at one end and for a very large trapping rate γ the rest (dimer) could be taken as decoupled. The exciton moves from the very beginning approximately in the dimer avoiding the place influenced by the sink. Analogously, in the hexagonal model of the photosynthetic unit the reaction center seems to be almost decoupled from the antenna system for a very large trapping rate γ. Still there is no doubt that after a long time the whole occupation probability $P(t)$ of the exciton disappears due to the trapping term.

In the last few years much attention has been paid to the problem of nonlinear interactions in coupled exciton-vibration systems.[14,15] A possible approach to it is the so-called discrete nonlinear Schrödinger equation (DNLSE, sometimes also called discrete self-trapping equation) which—though not yet rigorously justified—has the advantage of allowing for a simple modeling of the quasiparticle transfer. In this equation, besides the transfer-matrix element V, a nonlinear coupling constant χ describing the site energy lowering due to quasiparticle formation is contained. One encounters this equation in the context of modeling numerous phenomena from various fields of physics.

Although the DNLSE was already mentioned in early papers on the polaron problem (see, e.g., Ref. 13), and much physics has been extracted through numerical analysis,[14] exact solutions are not known in general.

However, it has been found recently, that considerable insight can be gained into essential physics of the system through the exact analytical solutions when the system has only two sites. This case of the nonlinear dimer has been investigated during the last few years from many points of view. Kenkre with his collaborators[15–19] and Szöcs and Bařnacky[20] have tackled the problem with the occupation probability difference as the most important quantity in mind. The exact time evolution for the occupation probability difference was given in terms of Jacobian elliptic functions for arbitrary initial conditions. Setting the occupation of the first site initially to one, the transition to a self-trapped state was obtained by Kenkre and Campbell[15] in a dimer with $\chi \geq 4V$. However, one-sided oscillations in the occupation difference appear for some initial conditions already for $\chi > 2V$. This can be related to the appearance of a homoclinic structure on the Bloch sphere, which was shown by Esser and Hennig.[21] For increasing χ the separatrix of this homoclinic structure grows and at $\chi = 4V$ starts to include the poles of the sphere which correspond to states completely localized at one of the sites.

Excitation transfer in trapless dimers and trimers can be described by Hamiltonian flows located on the surface of the Bloch sphere for the dimer and its higher-dimensional analog for the trimer case. This allows one to use the methods of nonlinear dynamics in the analysis of the transfer properties, in particular to prove the appearance of bifurcations in the flow-line pictures.[14,21] Esser with his collaborators[21,22] pointed out another interesting feature: the possibility of chaotic behavior due to a perturbation of the homoclinic structure which constitutes a route to chaos. In this case one has to leave the description of the problem in terms of occupation probabilities only and must include the evolution of all Bloch variables, i.e., one must follow precisely the time development of the non-diagonal elements of the corresponding density matrix.

For the dimer the limiting behavior for $t \rightarrow \infty$ has been treated with and without dissipation which was modeled in the framework of the stochastic Liouville equations with diagonal and nondiagonal Haken-Strobl parameters.[20] Attention has been paid to the influence of symmetry in the dimer, trimer, and n-mer. The DNLSE approach has also been used to consider the nonlinear trap problem by Dunlap and Kenkre[23] and Chen *et al.*,[24] in which impurities embedded in a linear host are modeled by a real nonlinear site energy containing the shift due to coupling to vibrations.

The aim of our contribution is to investigate the interplay between the nonlinearity and the trapping of the excitation. The trapping of the exciton is modeled by an imaginary part γ of the site is energy, which leads to a finite lifetime of the excitation. We shall follow the influence of both nonlinearity and trapping on the transfer properties. The paper is organized as follows. In Sec. II the formulation of the problem and the basic equations are given. Sections III and IV contain equations which describe the dynamics of a dimer and a trimer, respectively, including nonlinear coupling and the influence of a sink placed at one end of the configuration. We present their numerical solutions and derive some analytic expressions for the case of very strong trapping. In Sec. V conclusions are drawn.

II. FORMULATION OF THE MODEL AND BASIC EQUATIONS

A. The DNLSE

As the basic equation describing the excitation transfer in our systems we use the discrete nonlinear Schrödinger equation

$$i\frac{d}{dt}c_n(t)=(\varepsilon_n-\chi_n|c_n|^2)c_n+\sum_m V_{nm}c_m \ , \tag{1}$$

where c_n is the probability amplitude of the exciton to occupy the molecule at the nth site, ϵ_n is the exciton site energy, $V_{nm}(n \neq m)$ is the transfer-matrix element, and χ_n is the nonlinearity parameter describing the lowering of the site energy by exciton occupation. Introducing the density-matrix elements

$$\rho_{mn}(t) := c_m(t)c_n^*(t) \ , \tag{2}$$

we describe the system evolution by the density-matrix equation

$$i\frac{\partial}{\partial t}\rho_{nm}=(\epsilon_n-\epsilon_m)\rho_{nm}+\sum_k (V_{nk}\rho_{km}-\rho_{nk}V_{km}) \ . \tag{3}$$

Here

$$\epsilon_n := \varepsilon_n - \chi_n\rho_{nn} \tag{4}$$

is an effective site energy.

B. Influence of the sink

Trapping at a particular site s, consistent with the condition $\rho_{nn}(t) > 0$ for any time t, can be introduced into Eq. (3) by supplementing the right-hand side (rhs) with the terms

$$-i(\gamma/2)\rho_{ns} \quad (n \neq s) \tag{5}$$

for the nondiagonal and

$$-i\gamma\rho_{ss} \tag{6}$$

for the diagonal matrix elements connected with the trap site s. This description, which was called the full sink model, guarantees that the occupation probabilities are non-negative as was first shown in Ref. 7. It is equivalent to introducing into the Hamiltonian the matrix element $H_{ss} = -i\gamma/2$ for the sink place and replacing $\epsilon_n - \epsilon_m$ by $\epsilon_n - \epsilon_m^*$ in (3).

C. Perturbation theory for a large γ

In the case of a large trapping rate γ at site s, i.e., when γ exceeds by far all the other energies entering the rhs of Eq. (3), one can simplify the system (3)–(6) by assuming quasistationarity in the equations for matrix elements ρ_{mn} involving the trapping site. This corresponds to neglecting times smaller than γ^{-1} in the evolution of the

system and is formally achieved by setting $\dot{\rho}_{mn}=0$ for $m=s$ or $n=s(m\neq n)$ and $m=n=s$. This procedure is quite analogous to that used for the transition from the stochastic Liouville to the Pauli master equation in Ref. 5 when quasistationarity is assumed for the nondiagonal density-matrix elements due to the fast phase relaxation connected with the stochastic sources. Here we apply this approximation to only a part of the nondiagonal density-matrix elements, namely those connected with the trap site. As we will show, this results in analytical expressions for the density-matrix elements connected with the sink site in the case of large γ. One finds for the nondiagonal elements $n\neq s$

$$\rho_{ns}=\frac{1}{\epsilon_n-\epsilon_s-i(\gamma/2)}\sum_k(\rho_{nk}V_{ks}-V_{nk}\rho_{ks}) \tag{7}$$

and for the diagonal elements connected with the trap

$$\rho_{ss}=\frac{i}{\gamma}\sum_k(\rho_{sk}V_{ks}-V_{sk}\rho_{ks})\ . \tag{8}$$

From the rhs of Eq. (7) it is evident that the ρ_{ns} are of the order of the small parameter $(V/\gamma)\ll 1$ where V is the typical value for the transfer-matrix elements entering the rhs of (7), i.e., the sink site effectively decouples from the other sites. Evaluating (7) and (8) in this small parameter iteratively one obtains approximations to ρ_{ns} and ρ_{ss} for the case of large γ which complement our numerical results and are considered below. We shall now treat the dimer and the trimer separately.

III. THE DIMER WITH A SINK

A. Equations of motion

Restricting the transfer to the two sites of a dimer with $V_{12}=V_{21}=-V<0$ one arrives at

$$\begin{aligned}
i\dot{\rho}_{11}&=+V(\rho_{12}-\rho_{21})\ ,\\
i\dot{\rho}_{22}&=-V(\rho_{12}-\rho_{21})-i\gamma\rho_{22}\ ,\\
i\dot{\rho}_{12}&=+V(\rho_{11}-\rho_{22})-i(\gamma/2)\rho_{12}+(\epsilon_1-\epsilon_2)\rho_{12}\ ,\\
i\dot{\rho}_{21}&=-V(\rho_{11}-\rho_{22})-i(\gamma/2)\rho_{21}-(\epsilon_1-\epsilon_2)\rho_{21}\ .
\end{aligned} \tag{9}$$

Passing to the Bloch variables

$$\begin{aligned}
x_1&:=\rho_{12}+\rho_{21}\ ,\\
x_2&:=i(\rho_{12}-\rho_{21})\ ,\\
x_3&:=\rho_{11}-\rho_{22}\ ,
\end{aligned} \tag{10}$$

and introducing the norm as a separate variable

$$n:=\rho_{11}+\rho_{22}\ , \tag{11}$$

one obtains the equations of motion

$$\begin{aligned}
\dot{x}_1&=-(\gamma/2)x_1+\Delta\epsilon(t)x_2\ ,\\
\dot{x}_2&=-(\gamma/2)x_2-\Delta\epsilon(t)x_1+2Vx_3\ ,\\
\dot{x}_3&=-(\gamma/2)(x_3-n)-2Vx_2\ ,\\
\dot{n}&=-(\gamma/2)(n-x_3)
\end{aligned} \tag{12}$$

with $\Delta\epsilon(t):=(\epsilon_2-\epsilon_1)+\chi x_3$.

B. Previously obtained results

In the absence of trapping, i.e., for $\gamma=0$ the system (12) reduces to the nonlinear Bloch equations considered in Ref. 21. In this case, besides the energy, there is a second integral of the motion restricting the Bloch variable to the surface of a sphere.

In Ref. 21 the fixed points of the trapless system (12) were analyzed. One finds that for $\chi=2V$ a bifurcation is realized which follows for the symmetric dimer ($\epsilon_1=\epsilon_2$) from $\dot{x}_2=0$, i.e.,

$$(2V-\chi x_1)x_3=0\ . \tag{13}$$

For $\chi\leq 2V$ the only solution of Eq. (13) is given by $x_3=0$, whereas for $\chi>2V$ the new solution $x_1=2V/\chi$ appears, resulting in two fixed points with $x_2=0$, $x_3=\pm\sqrt{1-(2V/\chi)^2}$. These points correspond to the new ground states arising from the polaronic effect which holds the quasiparticle preferentially at one of the two sites of the dimer. The solution $x_3=0$ for $\chi>2V$ corresponds to an unstable hyperbolic point at the center of a separatrix. Into this homoclinic structure the new ground states are embedded.

Kenkre and Campbell were able to rewrite the system (12) into a closed equation for the probability difference $x_3=p(t)=P_1(t)-P_2(t)$. The analytical and numerical solution leads for the case of the localized initial condition $P_1(0)=1$ to the so-called self-trapped states for $\chi\geq 4V$.[15]

We now turn to investigating the influence of the nonlinearity on the trapping process of the exciton in the dimer. We shall point out changes in the dynamic properties due to the trapping rate γ.

C. Analytical results for strong trapping

From (7) and (8) we know that strong trapping leads to the expressions

$$\rho_{12}=\frac{V}{\epsilon_1-\epsilon_2-i(\gamma/2)}(\rho_{22}-\rho_{11}) \tag{14}$$

($\rho_{21}=\rho_{12}^*$) and

$$\rho_{22}=\frac{iV}{\gamma}(\rho_{12}-\rho_{21})\ , \tag{15}$$

from which an explicit expression for the occupation of the sink site ρ_{22} can be derived. In the case without nonlinearity ($\chi=0$) one finds

$$\rho_{22}^0=\frac{V^2}{(\epsilon_1-\epsilon_2)^2+(\gamma/2)^2}\rho_{11}^0\ , \tag{16}$$

which demonstrates that due to the strong trapping the occupation of the effectively decoupled sink site is very small, namely $\rho_{22}\sim(V/\gamma)^2\rho_{11}\ll\rho_{11}$. The effect of nonlinearity in the perturbation series for strong trapping is to modify the energy difference in the denominator:

$$\rho_{22}=\frac{V^2}{(\epsilon_1-\epsilon_2-\chi\rho_{11})^2+(\gamma/2)^2}\rho_{11}\ . \tag{17}$$

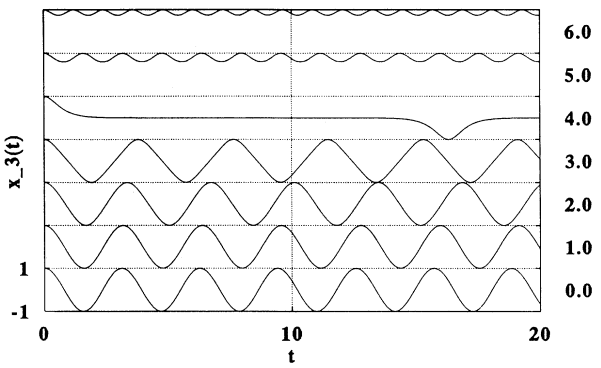

FIG. 1. Occupation probability difference $x_3(t)$ for the trapless dimer ($\gamma=0$) and various nonlinear coupling strengths χ (given to the right of the plots). The transition to a self-trapped state at site 1 ($x_3 \sim 1$) is obvious.

D. Numerical results

We have calculated the time dependence of the Bloch variables in the presence of nonlinearity and trapping by a direct numerical integration of the nonlinear equation (1) including the trapping as described in Sec. II B.

Our results are displayed in Figs. 1–4 for different trapping rates γ and various nonlinearity parameters χ. We have chosen for all figures a symmetric configuration ($\varepsilon_1=\varepsilon_2$) with $V=1$ and the initial condition $P_1(0)=1$.

In Fig. 1 the formation of a self-trapped state for $\chi \geq 4V$ is shown. The occupation difference oscillates between $x_3=-1$ and 1 with mean value zero for $\chi<4V$. For $\chi>4$ it remains in the vicinity of $x_3=1$, i.e., the exciton is preferentially located at site 1 of the dimer. For exactly $\chi=4V$ the initial condition $P_1(0)=1$ is located on the separatrix between trapped and detrapped states and approaches a very unstable hyperbolic fixed point[21] (due to the numerical inaccuracies the curve actually shown corresponds to χ a little bit below 4.0).

For both, γ and χ different from zero we show in parts (a) of Figs. 2–4 the time dependence of the total occupation probability $n(t)$ and in parts (b) the occupation difference $x_3(t)$ rescaled with the total occupation probability.

In Fig. 2 the influence of the small trapping rate $\gamma=0.5$ is displayed. The total occupation probability decays slowly. Strong nonlinearity ($\chi \geq 5$) leads to an effective switching off of the trapping. In this case the total occupation remains almost constant until $t > 10/V$.

In Fig. 3 the intermediate trapping rate $\gamma=2$ has been chosen. The lifetime of the exciton in this case is smaller than for the large trapping rate $\gamma=10$ (Fig. 4) and in-

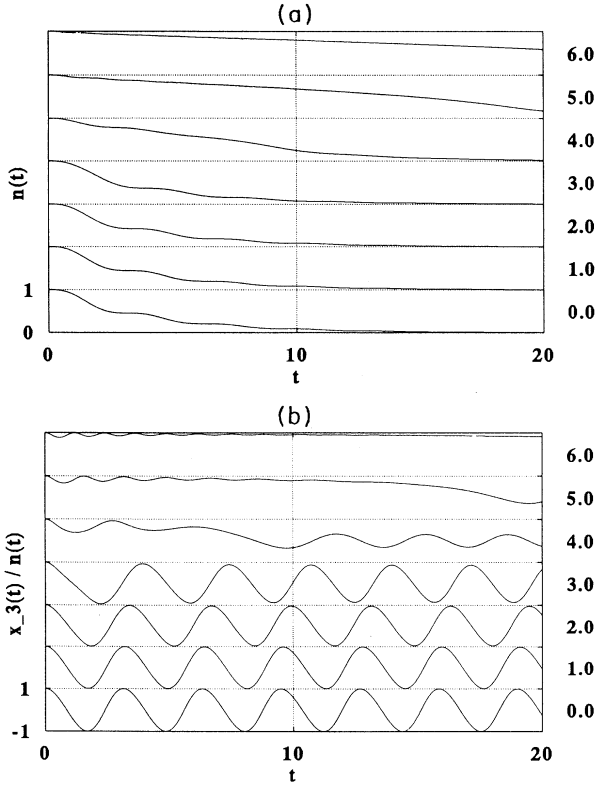

FIG. 2. Total occupation probability $n(t)$ (a) and normalized occupation probability difference $x_3(t)/n(t)$ (b) for a dimer with weak trapping $\gamma=0.5$ and various nonlinear coupling strengths χ (given to the right of the plots). Again the formation of a self-trapped state for $\chi \geq 4$ can be observed. It is, however, not stable and decays after some time ($t \sim 10$ for $\chi=4$).

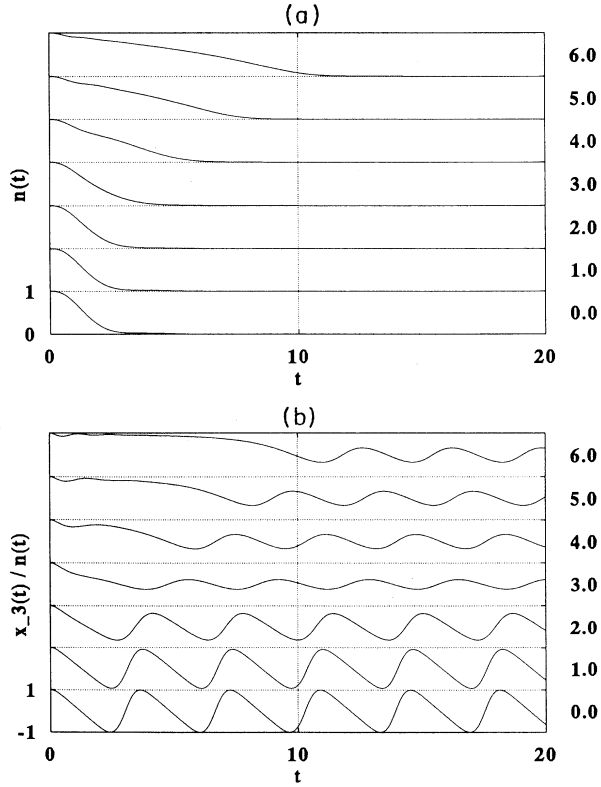

FIG. 3. Total occupation probability (a) and normalized occupation probability difference (b) for a dimer with intermediate trapping $\gamma=2.0$. The decay of the total occupation is faster than for $\gamma=0.5$. A tendency to form a self-trapped state can be recognized even for $\chi<4$, but it disappears earlier than for a small trapping rate.

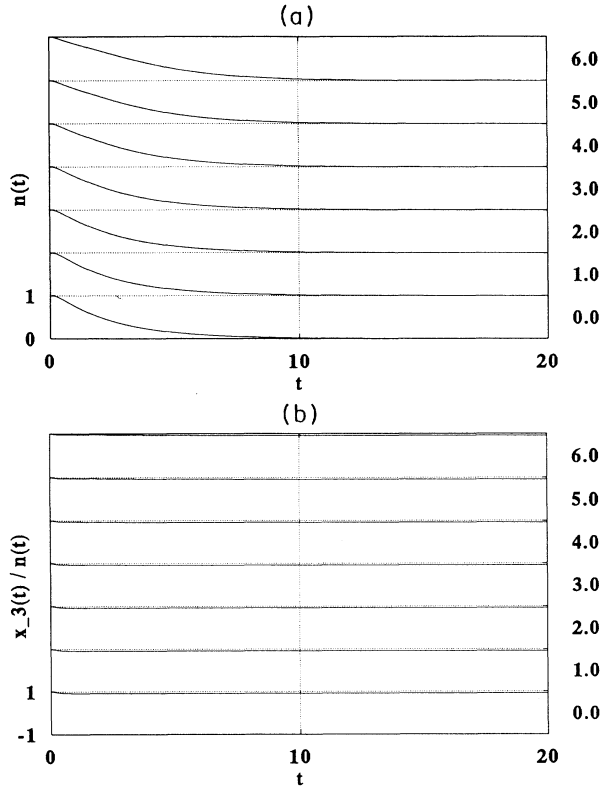

FIG. 4. Total occupation probability (a) and normalized occupation probability difference (b) for a dimer with very strong trapping $\gamma=10$. The total occupation falls off slower than for intermediate trapping rates. The oscillations of the occupation differences have disappeared and the exciton is almost completely localized at site 1. The influence of the nonlinear coupling is very small.

creases further as the trapping becomes stronger. This is due to the effective decoupling of the sink site which becomes important for $\gamma>4$. It leads to a very large difference in the occupation probabilities of the sites 1 and 2.

A concise inspection of the probability difference $P_1(t)-P_2(t)$, scaled to the whole occupation probability [Figs. 2(b)–4(b)] reveals, that for growing trapping strength the transition to the self-trapped state takes place for $\chi<4V$ already [but compare Fig. 2(b) in the paper by Tsironis, Kenkre, and Finley[16]]. It is formed at the beginning of the time development and after some time it disappears. The self-trapped state is not stable because the whole probability decays completely [$P(t)\rightarrow 0$ for $t\rightarrow\infty$]. Self-trapping leads to a considerable enhancement of the lifetime of the exciton, e.g., for intermediate trapping rates (Fig. 3) and strong nonlinearity $\chi=6$ it is approximately four times longer than in the linear case $\chi=0$.

A very large trapping rate removes the influence of the nonlinearity almost completely (Fig. 4). The transfer probabilities for the exciton are reduced so much, that the occupation probability $P_2(t)$ is very low and the decay of the whole occupation probability $P(t)$ is almost independent on the nonlinearity parameter χ.

IV. THE TRIMER WITH A SINK

A. Previously obtained results

In the past some attention has been given to the solution of the nonlinear Schrödinger equation for the trimer. Preferentially symmetric trimers with symmetric initial conditions have been studied.

Eilbeck, Lomdahl, and Scott investigated the stationary solutions of the symmetric cyclic trimer (Fig. 2 in Ref. 14). They derived a bifurcation point and discussed the stability of the obtained solutions. Kenkre with his collaborators were able to obtain an equation for the probability difference $x_3=p(t)=P_1(t)-2P_2(t)$ for a symmetric trimer with symmetric initial conditions.[18]

B. Equations of motion

We consider a trimer (chain of three sites) with $V_{12}=V_{21}=-V$ and $V_{23}=V_{32}=-V'<0$. A sink is introduced at site 3. Similarly to the case of the dimer one can pass to generalized Bloch variables x_{1-8} containing also the variables x_{1-3} which were previously introduced for the dimer. The procedure of introducing the generalized variables x_{1-8} is explained in the Appendix. One obtains

$$
\begin{aligned}
x_1&:=\rho_{12}+\rho_{21}\ ,\\
x_2&:=i(\rho_{12}-\rho_{21})\ ,\\
x_3&:=\rho_{11}-\rho_{22}\ ,\\
x_4&:=\rho_{31}+\rho_{13}\ ,\\
x_5&:=i(\rho_{13}-\rho_{31})\ ,\\
x_6&:=\rho_{23}+\rho_{32}\ ,\\
x_7&:=i(\rho_{23}-\rho_{32})\ ,\\
x_8&:=\rho_{11}-\rho_{33}\ ,\\
x_9&:=\rho_{22}-\rho_{33}\ ,\\
n&:=\rho_{11}+\rho_{22}\ ,\\
N&:=\rho_{11}+\rho_{22}+\rho_{33}\ .
\end{aligned}
\tag{18}
$$

In addition to a set of linearly independent variables we have introduced $x_9=x_8-x_3$ as well as the occupation sum of the sites 1 and 2, n and the total trimer occupation N. The variable n will be useful for considering the sink influence at site 3. We obtain the generalized system of Bloch equations

$$
\begin{aligned}
\dot{x}_1&=+(\epsilon_2-\epsilon_1)x_2-V'x_5\ ,\\
\dot{x}_2&=+(\epsilon_1-\epsilon_2)x_1+V'x_4+2Vx_3\ ,\\
\dot{x}_3&=-2Vx_2+V'x_7\ ,\\
\dot{x}_4&=+(\epsilon_3-\epsilon_1)x_5+Vx_7-V'x_2-(\gamma/2)x_4\ ,\\
\dot{x}_5&=+(\epsilon_1-\epsilon_3)x_4-Vx_6+V'x_1-(\gamma/2)x_5\ ,\\
\dot{x}_6&=+(\epsilon_3-\epsilon_2)x_7+Vx_5-(\gamma/2)x_6\ ,
\end{aligned}
\tag{19}
$$

$$\dot{x}_7 = +(\epsilon_2-\epsilon_3)x_6 - Vx_4 + 2V'x_9 - (\gamma/2)x_7 ,$$
$$\dot{x}_8 = -Vx_2 + V'x_7 - (\gamma/3)(N-x_8-x_9) ,$$
$$\dot{x}_9 = +Vx_2 + 2V'x_7 - (\gamma/3)(N-x_8-x_9) ,$$
$$\dot{n} = -V'x_7 ,$$
$$\dot{N} = -(\gamma/3)(N-x_8-x_9) .$$

C. Analytical results for strong trapping

According to (7) and (8) strong trapping leads to

$$\rho_{13} = \frac{1}{\epsilon_1-\epsilon_3-i(\gamma/2)}(V\rho_{23}-V'\rho_{12}) , \tag{20}$$

$$\rho_{23} = \frac{1}{\epsilon_2-\epsilon_3-i(\gamma/2)}(V'\rho_{33}-V'\rho_{22}+V\rho_{13}) , \tag{21}$$

and

$$\rho_{33} = \frac{iV'}{\gamma}(\rho_{23}-\rho_{32}) . \tag{22}$$

This means that all density-matrix elements with one index 3 are of the order $O(V/\gamma)$ and therefore small, ρ_{33} is even of order $O(V^2/\gamma^2)$. Keeping only terms of leading order one can express x_{4-7} through x_{1-3} and obtain a closed system of equations for the latter:

$$\dot{x}_1 = -(\tilde{\gamma}/2)x_1 + (\epsilon_2-\epsilon_1)x_2 ,$$
$$\dot{x}_2 = -(\tilde{\gamma}/2)x_2 - (\epsilon_2-\epsilon_1)x_1 + 2Vx_3 , \tag{23}$$
$$\dot{x}_3 = -(\tilde{\gamma}/2)(x_3-n) - 2Vx_2 ,$$
$$\dot{n} = -(\tilde{\gamma}/2)(n-x_3) .$$

Comparing this to (12) we notice that the equations of motion for the trimer reduce for very strong trapping to the dimer equations with the effective sink rate

$$\tilde{\gamma} := \frac{(2V')^2}{\gamma} . \tag{24}$$

The effective sink rate $\tilde{\gamma}$ in Eq. (24) becomes small compared to V' for $\gamma \gg V'$ and this shows again that the sink site in the trimer is effectively decoupled in this case.

D. Numerical results

We have calculated numerically the time dependence of the site occupation probabilities in the presence of trapping and of a nonlinearity. With respect to the nonlinearity we consider two different cases:

Configuration (I): The nonlinearity χ is the same for all three sites;

Configuration (II): The sink site is linear, i.e., $\chi_1=\chi_2=\chi, \chi_3=0$. Our data were obtained through a numerical integration of the nonlinear Schrödinger equation (1). We have chosen for all figures $V=1$ and the initial condition $P_1(0)=1$. The sink influences site 3. In the analysis we will concentrate on self-trapping, the decoupling of the sink site for large γ and regular vs chaotic time dependences.

A moderate nonlinearity (up to $\chi \sim 2$) has little influence on the decay of the exciton (Fig. 5). As for the

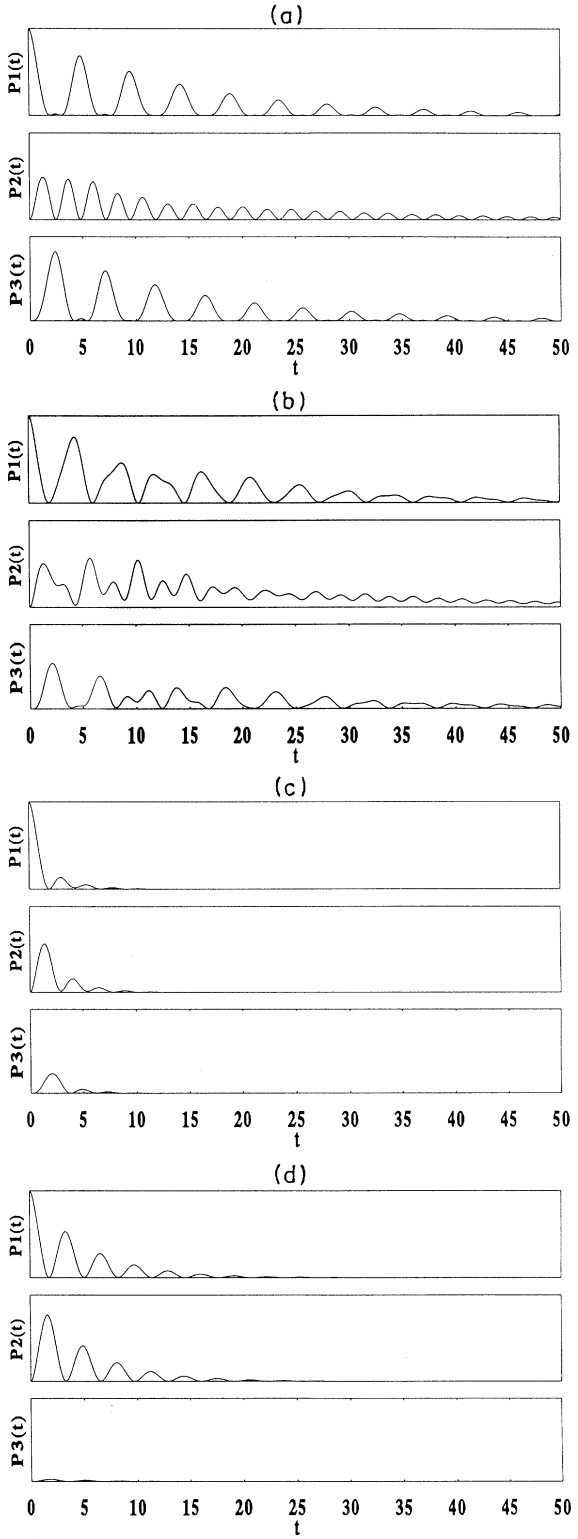

FIG. 5. Decay of an exciton on a trimer with small nonlinear coupling $\chi=2.0$ for different sink rates and configurations: (a) $\gamma=0.2$, conf. (I); (b) $\gamma=0.2$, conf. (II); (c) $\gamma=2$; (d) $\gamma=10$, both conf. (I). Conf. (II) shows irregular behavior for a small sink rate due to the destruction of symmetry (b). For a larger sink rate conf. (II) is not displayed because it behaves very similar to conf. (I). Comparison of (c) and (d) shows the decoupling of the sink site for large γ.

linear trimer (not displayed), an intermediate trapping rate $\gamma=2$ [Fig. 5(c)] makes the decay faster than for weak trapping [Figs. 5(a) and 5(b)]. The decoupling of the sink site controls the behavior for a large trapping rate [Fig. 5(d)] and in this case there is not much difference between the two configurations (I) and (II, not displayed) because the occupation of site 3 is reduced so much. In contrast, for weak trapping the regular oscillations of type (I) change into quite an irregular behavior for configuration (II). This effect is also present without the trap (not displayed) and is obviously due to the destruction of the symmetry between the sites 1 and 3.

As one increases the nonlinearity further, a significant change of the behavior towards a self-trapped solution occurs. We discuss this first for the symmetric trimer of configuration (I) without trap. The regular behavior up to $\chi=2$ [Fig. 6(a)] is replaced by a rather chaotic one for $\chi=3$ [Fig. 6(b)]. Still the average occupation probabilities are approximately the same for all three sites. There is, however, a large interval where the occupation of site 3 is very small. For $\chi=4$ [6(c)] the transition to a self-trapped state on the dimer has occurred and the occupation of site 3 remains small all the time. The appearance of the time dependence is much more regular than close to the transition point in Fig. 6(b). A further increase of the nonlinearity parameter to $\chi\geq 5$ causes the exciton to be completely localized at site 1 [Fig. 6(d)], after that no other qualitative changes occur, just frequency and amplitude of the small oscillations in the occupation probabilities slightly depend on χ (not displayed). The consecutive transitions can be explained by the bifurcations which the stationary solutions undergo as the nonlinearity changes. They have been discussed in Ref. 14 in detail for the nonlinear Schrödinger equation without sinks.

Figure 7 shows that the bifurcations are still present for a small trap strength $\gamma=0.2$ [cf. also Figs. 5(a) and 5(b)]. In the symmetric configuration (I) the transition to self-trapping on the dimer occurs for all sink rates later than in configuration (II). We illustrate this with Figs. 7(a) and 7(b). The effect can be understood having in mind that equal site occupation probabilities for the asymmetric configuration (II) cause a shift in the effective site energies ϵ_i, on the dimer which in turn obstructs the transition from the dimer to site 3. The transition to self-trapping on site 1 is not affected by the two different configurations (not displayed).

Even for very large γ there is a clear transition from dynamic localization involving equally two sites of the subdimer to a solution completely localized at site 1 due to nonlinear self-trapping [Figs. 5(d) and 8]. In this case, however, the occupation probability on site 3 is always small. This is not due to nonlinearity-induced self-trapping but to the decoupling of the sink site. In general, both effects work together in slowing down the decay of the excitation. The lifetime is, e.g., for $\gamma=10$ and $\chi=5$ doubled in comparison to $\chi=3$.

The formation of self-trapped states due to nonlinearity is not stable for $\gamma>0$: as the total occupation probability becomes small with increasing time the effect disappears and the site occupation probabilities level out, as it can be seen, e.g., from Fig. 7(b) ($t>35$) and Fig. 8(b) ($t>30$).

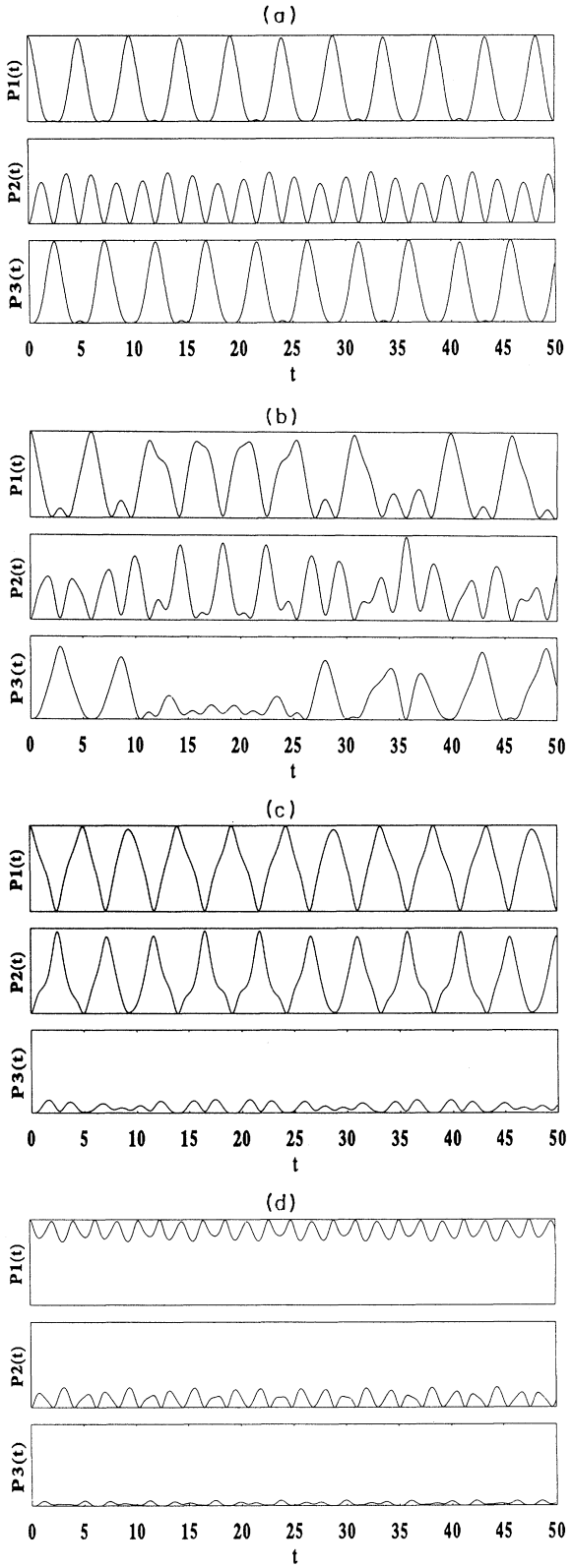

FIG. 6. The formation of a self-trapped state for the trapless symmetric trimer [conf. (II), $\gamma=0$]. At $\chi=2$ (a) the behavior is very similar to the linear trimer. The time dependence becomes irregular for $\chi=3$ (b). For $\chi=4$ (c) the solution is localized on a subdimer and for $\chi=5$ (d) on site 1.

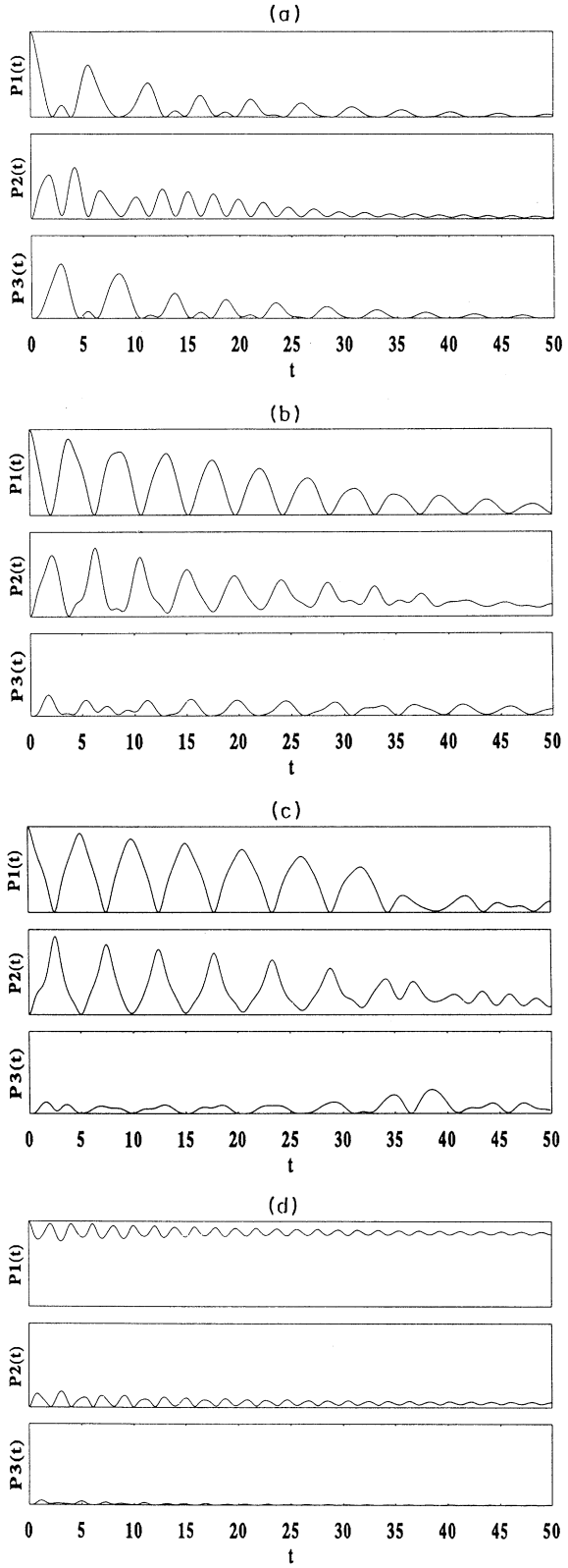

FIG. 7. Formation of a self-trapped state for a trimer with the small sink rate $\gamma=0.2$: (a) $\chi=3$, conf. (I), (b) $\chi=3$, conf. (II), (c) $\chi=4$, and (d) $\chi=5$, both conf. (I). For conf. (II) self-trapping on the dimer occurs for smaller nonlinearities. The self-trapped state on the dimer in (c) disappears for $t \geq 35$.

The nonlinearity effects must decrease for large time since the occupation probabilities entering the effective site energies (4) then become negligibly small.

In contrast, the lowering of the occupation ρ_{33} due to strong trapping does not depend on time. The sink site is almost decoupled and the behavior of P_1 and P_2 can be interpreted as a perturbed dimer [Figs. 5(d), 8(a), and 8(b)]. We note the interesting effect, that the time dependence looks quite regular as well for $\chi \leq 3$ [Fig. 5(d)] as for $\chi \geq 5$ [Fig. 8(b)] but much more chaotic for $\chi=4$ [Fig. 8(a)]. We relate this to the fact, that for $\chi=4$ the initial condition $P_1(0)=1$ is just on the homoclinic orbit (cf. Fig. 1) which encloses the self-trapped states for the system without trap. Time evolution will therefore take the system in the perturbed dimer very close to the hyperbolic fixed point where it is very unstable and as a result one observes chaos (see Ref. 21).

In the last Fig. 9 we present a numerical check for Eq. (24). We compare the time evolution for a trimer with the large sink rate $\gamma=10$ (full lines) to a dimer with $\gamma=0.4$ (dots) according to this equation. We find good agreement in particular for $\chi=0$ (a). For $\chi=3$ the result is still reasonable, but not as good as in (a) since (24) was derived also under the assumption $\gamma \gg \chi$.

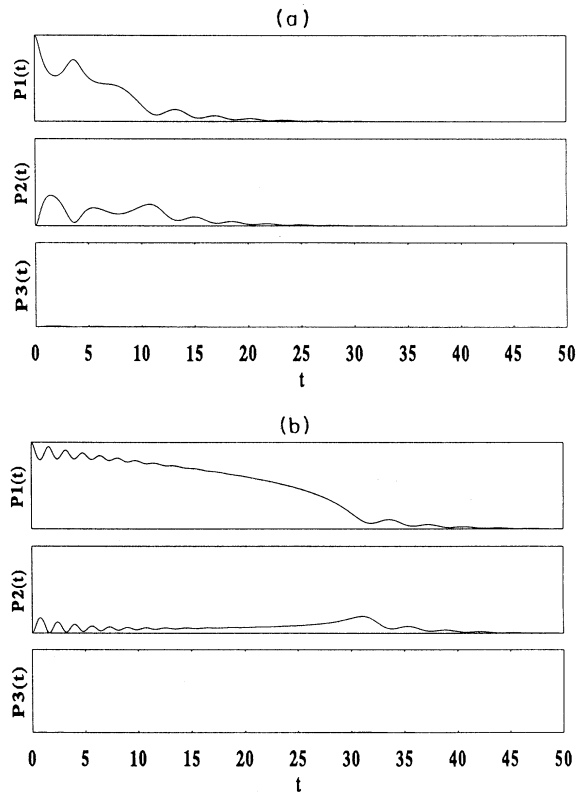

FIG. 8. Transition to a self-trapped solution on site 1 for strong trapping $\gamma=10$. The nonlinear coupling is (a) $\chi=4$ and (b) $\chi=5$. The self-trapped state is unstable for $t \geq 30$. The occupation of site 3 is always very small, it is effectively decoupled. The time dependence for $\chi=4$ is very irregular.

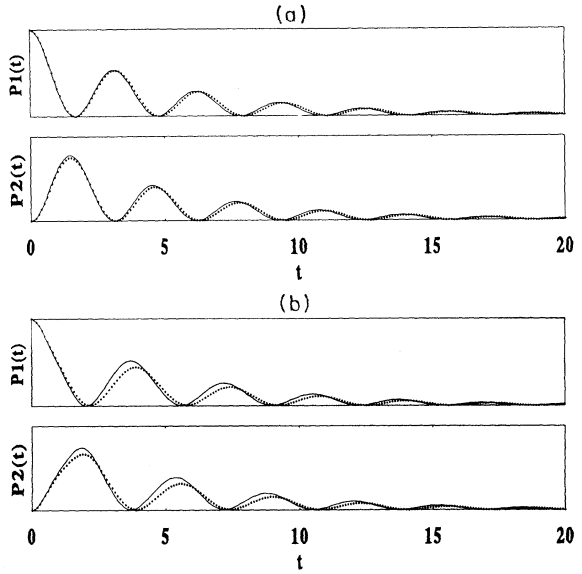

FIG. 9. Reduction of the trimer with strong trapping to an effective dimer with weak trapping. The full line shows the occupation probabilities of the sites 1 and 2 for a trimer with $\gamma=10$ and (a) $\chi=0$, (b) $\chi=3$. The dots show according to Eq. (24) the corresponding effective dimer with the sink rate $\gamma=0.4$.

V. CONCLUSIONS

In the present paper we studied the combined effect of trapping due to a sink and transport nonlinearity due to excitonic-vibronic interactions on the transfer dynamics and the lifetime of an exciton. The specific systems we have analyzed were the dimer and the trimer with a chain topology. A sink was introduced at one end of the configuration using the formalism given in Ref. 7. The initial condition for the numerical integration of the DNLSE was always a state localized at the end opposite to the sink site.

The main effect of the nonlinearity is self-trapping. In the dimer with sink a tendency to form a self-trapped state could be observed for $\chi<4V$, i.e., for smaller nonlinearity than in the isolated dimer. In the trimer self-trapping on the sinkless subdimer for an intermediate nonlinearity was found besides states which are localized on one site only for strong nonlinearity. The transition to a self-trapped state was accompanied by relatively irregular time dependencies. Though self-trapping was enhanced by the sink for short times, the decay of the total occupation probability destroyed the localized states for long times. Self-trapping was shown to have a crucial influence on the lifetime of the excitation which grows for increasing nonlinearity.

For large sink rates the sink site becomes effectively decoupled as it was shown using an asymptotic approximation and in this case the occupation of the sink site is reduced so much that the lifetime even increases with growing sink rate. For small trapping rates there was a clear change in the behavior when the nonlinearity of the sink was dropped, while this effect was suppressed by the effective decoupling of this site for strong trapping.

ACKNOWLEDGMENTS

Support by the Deutsche Forschungsgemeinschaft (DFG) is gratefully acknowledged. One of us (I.B.) wishes to thank the Deutscher Akademischer Austauschdienst (DAAD) for support and the Humboldt University, Berlin for the kind hospitality.

APPENDIX: GENERALIZED BLOCH REPRESENTATION FOR THE TRIMER

The Bloch variables for the dimer are derived from the state vector $\underline{c}=(c_1,c_2)^T$ by employing the Pauli matrices σ_i

$$\sigma_1=\begin{bmatrix}0&1\\1&0\end{bmatrix},\quad \sigma_2=\begin{bmatrix}0&-i\\i&0\end{bmatrix},\quad \sigma_3=\begin{bmatrix}1&0\\0&-1\end{bmatrix}, \tag{A1}$$

which are the generators of the Lie algebra SU(2). In this case one defines

$$x_i:=\underline{c}^+\sigma_i\underline{c}\quad (i=1,2,3)\,. \tag{A2}$$

Analogously, one derives generalized Bloch variables for the trimer from the state vector $\underline{c}=(c_1,c_2,c_3)^T$ using the Gell-Mann matrices λ_i, which are generators of the Lie algebra SU(3), in the form

$$\lambda_1=\begin{bmatrix}0&1&0\\1&0&0\\0&0&0\end{bmatrix},\quad \lambda_2=\begin{bmatrix}0&-i&0\\i&0&0\\0&0&0\end{bmatrix},\quad \lambda_3=\begin{bmatrix}1&0&0\\0&-1&0\\0&0&0\end{bmatrix},$$
$$\lambda_4=\begin{bmatrix}0&0&1\\0&0&0\\1&0&0\end{bmatrix},\quad \lambda_5=\begin{bmatrix}0&0&-i\\0&0&0\\i&0&0\end{bmatrix},\quad \lambda_6=\begin{bmatrix}0&0&0\\0&0&1\\0&1&0\end{bmatrix}, \tag{A3}$$
$$\lambda_7=\begin{bmatrix}0&0&0\\0&0&-i\\0&i&0\end{bmatrix},\quad \lambda_8=\begin{bmatrix}1&0&0\\0&0&0\\0&0&-1\end{bmatrix},\quad \lambda_9=\begin{bmatrix}0&0&0\\0&1&0\\0&0&-1\end{bmatrix}.$$

They generate the variables

$$x_i:=\underline{c}^+\lambda_i\underline{c}\quad (i=1,\ldots,9)\,. \tag{A4}$$

These variables x_i are by definition real. We have chosen λ_8 in a modified form convenient for our calculations and added λ_9 which is linearly dependent ($\lambda_9=\lambda_8-\lambda_3$). Our variables x_8 and x_9 are therefore generalizations of the variables x_3 and have the form of differences between occupation probabilities.

*Electronic address: barvik@ns.karlov.mff.cuni.cz
†Electronic address: schanz@summa.physik.hu-berlin.de

[1]H. Haken and P. Reineker, in *Excitons, Magnons and Phonons in Molecular Crystals,* edited by A. B. Zahlan (Cambridge University Press, Cambridge, 1968), p. 185.
[2]M. Grover and R. Silbey, J. Chem. Phys. **52**, 2099 (1970); **54**, 4843 (1971).
[3]V. M. Kenkre, in *Exciton Dynamics in Molecular Crystals and Aggregates,* edited by G. Höhler, Springer Tracts in Modern Physics 94 (Springer, Berlin, 1982), pp. 1–109.
[4]P. Reineker, in *Excitation Dynamics in Molecular Crystals and Aggregates* (Ref. 3), pp. 111–226.
[5]P. Reineker and R. Kühne, Z. Phys. B **22**, 193 (1975); R. Kühne and P. Reineker, *ibid.* **22**, 201 (1975).
[6]V. M. Kenkre, E. W. Montroll, and M. F. Shlesinger, J. Stat. Phys. **9**, 45 (1973).
[7]V. Čápek and V. Szöcs, Phys. Status Solidi B **125**, K 137 (1984).
[8]V. Szöcs and I. Barvík, J. Theor. Biol. **122**, 179 (1986).
[9]I. Barvík, in *Dynamical Processes in Condensed Molecular Systems,* edited by A. Blumen (World Scientific, Singapore, 1991), pp. 275–287.
[10]I. Barvík, in *Large Scale Molecular Systems,* Vol. 258 of NATO ASI Series, edited by W. Gans, A. Blumen, and A. Amann (Plenum, New York, 1991), pp. 371–374.
[11]P. Chvosta and I. Barvík, Z. Phys. B **85**, 227 (1991).
[12]P. Heřman and I. Barvík, Phys. Lett. A **163**, 313 (1992); I. Barvík and P. Heřman, Phys. Rev. B **45**, 2772 (1992); **47**, 2772 (1993).
[13]J. Appel, in *Solid State Physics: Advances in Research and Applications,* edited by F. Seitz, D. Turnbull, and H. Ehrenreich (Academic, New York, 1968), Vol. 21, p. 193.
[14]J. C. Eilbeck, P. S. Lomdahl, and A. C. Scott, Physica **16D**, 318 (1985).
[15]V. M. Kenkre and D. K. Campbell, Phys. Rev. B **34**, 4959 (1986).
[16]V. M. Kenkre and G. P. Tsironis, Phys. Rev. B **35**, 1473 (1987); G. P. Tsironis, V. M. Kenkre, and D. Finley, Phys. Rev. A **37**, 4474 (1988); G. P. Tsironis and V. M. Kenkre, Phys. Lett. A **127**, 209 (1988).
[17]V. M. Kenkre and H.-L. Wu, Phys. Lett. A **135**, 120 (1989); Phys. Rev. B **39**, 6907 (1989); H.-L. Wu and V. M. Kenkre, *ibid.* **39**, 2664 (1989); P. Grigolini, H.-L. Wu, and V. M. Kenkre, *ibid.* **40**, 7045 (1989).
[18]J. D. Andersen and V. M. Kenkre, Phys. Status Solidi B **177**, 397 (1993); Phys. Rev. B **47**, 11 134 (1993).
[19]V. M. Kenkre and M. Kus, Phys. Rev. B **46**, 13 792 (1992); **49**, 5956 (1994).
[20]V. Szöcs, P. Baňacký, and A. Zajac, Phys. Rev. A **42**, 737 (1990); V. Szöcs and P. Baňacký, *ibid.* **45**, 5415 (1992).
[21]B. Esser and D. Hennig, Z. Phys. B **83**, 285 (1991); Philos. Mag. B **65**, 887 (1992); D. Hennig and B. Esser, Phys. Rev. A **46**, 4569 (1992); D. Hennig, J. Phys. A **25**, 1247 (1992).
[22]B. Esser and H. Schanz, Chaos, Solitons Fractals **4**, 2067 (1994); Z. Phys. B **96**, 553 (1995).
[23]D. H. Dunlap and V. M. Kenkre, Phys. Rev. B **47**, 14 842 (1993).
[24]D. Chen, M. I. Molina, and G. P. Tsironis, J. Phys. Condens. Matter **5**, 8689 (1993).